Ab initio study of antiferromagnetic rutile-type FeF_2

G. Valerio and M. Catti
Dipartimento di Chimica Fisica ed Elettrochimica, Università di Milano, via Golgi 19, 20133 Milano, Italy

R. Dovesi and R. Orlando
Dipartimento di Chimica Inorganica, Fisica e dei Materiali, Università di Torino, via Giuria 5, 10125 Torino, Italy
(Received 17 March 1995)

The periodic unrestricted Hartree-Fock method has been used to calculate the ground-state spin-polarized wave function and total energy of tetragonal FeF_2. Contracted Gaussian-type functions represent the atomic orbitals of Fe and F atoms. The nature of the antiferromagnetic insulator, with a *d-d* type band gap, is reproduced correctly by the calculations. On the basis of the density of electron states, Mulliken population data, and charge- and spin-density maps, the $d_{xy}^2/d_{xz}^1 d_{yz}^1$ splitting of t_{2g}^4 states is proved for the Fe^{2+} ion, consistent with the Jahn-Teller distortion of the FeF_6 octahedron. A limited charge back transfer from F^- to Fe^{2+} is observed, with $z_{Fe} = +1.84|e|$. The equilibrium structural configuration and its evolution with pressure up to 12 GPa have been calculated, including internal relaxation. The athermal equation of state, structural, and elastic parameters show a good agreement with experimental data.

INTRODUCTION

Powerful computational tools have been made available in the past few years for simulating *ab initio* ground-state electronic and magnetic properties of crystalline transition-metal salts, to which a large number of materials useful for technological applications belong. Two approaches are very successful: the periodic Hartree-Fock scheme,[1] where the exchange part of electron-electron interaction is treated exactly and the correlation part is neglected, and the DFT-LSDA-LAPW (density-functional theory–local spin-density approximation –linearized augmented plane wave) method, taking into account both the exchange and the correlation effects on an approximate basis.[2] The former one is adopted in this study in the UHF (unrestricted Hartree-Fock) version,[3] which allows us to deal with crystalline systems containing open-shell ions.

Some fluorides of first-row transition metals with the rutile-type tetragonal structure (MnF_2, NiF_2, FeF_2) have been already investigated by the LSDA approximation.[4,5] However, it was necessary to introduce a higher level of sophistication (GGA, or generalized-gradient approximation)[5] in order to reproduce the insulating nature of FeF_2 correctly. On the other hand, with the UHF scheme, only oxides of transition metals with no orbital degeneracy ($t_{2g}^3 e_g^2$, $t_{2g}^3 e_g^0$ or $t_{2g}^6 e_g^2$ configuration) have been studied so far, i.e., MnO,NiO, and VO (Refs. 6,7), Fe_2O_3 (Ref. 8), and $KNiF_3$ (Ref. 9). The case of FeF_2 is more complex, because the $t_{2g}^4 e_g^2$ configuration in Fe^{2+} in octahedral surrounding requires a Jahn-Teller distortion in order to lift the threefold degeneracy of the t_{2g} level and produce an insulating state.[10] Thus, it is important to examine this solid compound by the UHF method as a test to assess its ability to deal with systems showing orbital degeneracy.

The structural properties and phase transitions of rutilelike difluorides can also be studied very conveniently by this theoretical approach. This has been already partly done for MgF_2,[11] and is particularly interesting in the case of FeF_2 for which experimental data concerning the structural evolution with pressure and the transition to a fluorite-type phase are available.[12] Further, iron difluoride is known to be antiferromagnetic below 78 K, and this magnetic behavior is a challenging feature to simulate theoretically, owing to the low Néel temperature.

COMPUTATION

The CRYSTAL92 code,[1] based on the *ab initio* periodic linear combination of atomic orbitals Hartree-Fock method, was used, with the supplementary option for unrestricted treatment of the spin-dependent part of the wave function in open-shell systems.[3] The latter feature is necessary to obtain spin-polarized eigenfunctions of the Fock Hamiltonian, because of the presence of four unpaired 3*d* electrons in isolated Fe^{2+} ions. The radial factors of atomic orbitals are expressed as linear combinations of Gaussian-type functions of the electron-nucleus distance. All electron basis sets were employed for both the F and Fe atoms, in the form of 18 and 27 atomic orbitals, respectively. The fluorine basis set, denoted as 7-311G* (Ref. 13), was taken from a previous study of MgF_2,[11] except for the addition of a *d* shell; its exponent was optimized, together with that of the outermost 4*sp* shell, so as to minimize the energy of crystalline FeF_2 (0.30 and 0.194 $bohr^{-2}$, respectively, were obtained). Iron was represented by a 8-6-411G* contraction with two *d*-type (41G) shells, similar to that utilized for α-Fe_2O_3,[8] but with exponents and coefficients reoptimized variationally on the isolated Fe^{2+} ion, because of the different valence state. The exponents of the 5*sp* and 4*d* shells of Fe were refined by searching for the minimum

0163-1829/95/52(4)/2422(6)/$06.00

TABLE I. Exponents (bohr^{-2}) and contraction coefficients of the (individually normalized) Gaussian functions adopted for Fe(II) in the present study. $y[\pm z]$ stands for $y\times10^{\pm z}$.

Shell type	Exponents	Coefficients	
		s	*p,d*
1*s*	3.161[+5]	2.270[−4]	
	4.520[+4]	1.929[−3]	
	9.628[+3]	1.110[−2]	
	2.522[+3]	5.000[−2]	
	7.602[+2]	1.705[−1]	
	2.630[+2]	3.691[−1]	
	1.029[+2]	4.034[−1]	
	4.294[+1]	1.434[−1]	
2*sp*	7.980[+2]	−5.200[−3]	8.500[−3]
	1.910[+2]	−6.810[−2]	6.090[−2]
	6.361[+1]	−1.313[−1]	2.116[−1]
	2.534[+1]	2.522[−1]	3.942[−1]
	1.073[+1]	6.420[−1]	3.975[−1]
	3.757[+1]	2.833[−1]	2.230[−1]
3*sp*	4.751[+1]	1.200[−2]	−2.170[−2]
	1.735[+1]	−2.339[−1]	−8.300[−2]
	6.981	−8.801[−1]	1.988[−1]
	3.073	9.954[−1]	1.285
4*sp*	1.294	1.0	1.0
5*sp*	5.306[−1]	1.0	1.0
3*d*	2.901[+1]		5.704[−2]
	8.043		2.635[−1]
	2.709		5.236[−1]
	9.412[−1]		5.491[−1]
4*d*	3.150[−1]		1.0

total crystal energy of FeF_2, as in the case of F. The parameters of the Fe basis set are reported in Table I.

The level of numerical approximation in evaluating the Coulomb and exchange series appearing in the SCF equations for periodic systems is controlled by five tolerances.[1] These are related to estimates of overlap or penetration for integrals of Gaussian functions on different centers, which define cutoff limits for series summation. The values used in the present calculations are 10^{-6}, 10^{-6}, 10^{-6}, 10^{-7}, and 10^{-13}. The reciprocal space was sampled according to a regular sublattice defined by 21 points in the irreducible Brillouin zone.

MAGNETIC AND STRUCTURAL BEHAVIOR

Antiferromagnetic state

FeF_2 is known to be antiferromagnetic (AF) below $T_N=78$ K (Ref. 14). In the corresponding magnetic structure, the two Fe^{2+} ions per unit cell (at 0, 0, 0 and $\frac{1}{2}$, $\frac{1}{2}$, $\frac{1}{2}$) have their spins oppositely aligned to each other and parallel to the tetragonal axis, so that they become symmetry independent and the space group changes from $P4_2/mnm$ to $Cmmm$. The centered orthorhombic cell is obtained by the (1-10/110/001) transformation, but the primitive unit cell is unvaried. We define the Fe1 atom (at 0, 0, 0) as having a net excess of α (spin-up) over β (spin-down) electrons, amounting ideally to four units with a magnetic moment of $4\mu_B$; the α and β populations of Fe2 are exactly exchanged. We shall often refer below to α and β electrons of Fe1, understanding actually electrons with majority (α of Fe1 and β of Fe2) and minority (β of Fe1 and α of Fe2) spins, respectively. A hypothetical ferromagnetic (FM) structure is considered, too, where Fe1 and Fe2 have the same α-β positive excess of four electrons, and the $P4_2/mnm$ symmetry is retained. Calculations of the ground-state wave function and total energy were carried out at the experimental crystal structure[15] with both the AF and FM configurations. The difference n_α-n_β electrons per primitive cell was constrained to be 0 or 8 in the AF or FM case, respectively, but the spin density, and then the ensuing atomic spin populations, were of course self-consistently refined in the SCF cycles. The energy difference ΔE(AF-FM) amounts to -1.55×10^{-4} hartree ($=-0.0042$ eV) per two formula units; therefore, the observed stability of the antiferromagnetic structure is confirmed by the theoretical UHF result at the athermal limit. Let us assume that the Ising-model relation $\Delta E=-2S^2Jz$ (Ref. 16) between ΔE(AF-FM) and the magnetic coupling constant J holds in this case, where S is the total spin moment ($=2$) and z is the metal-metal coordination number ($=8$). Then, the value $J/k_B=0.8$ K is obtained, which may be compared with experimental results ranging between 2.75 and 3.03 K (Ref. 17). Some underestimate is observed for the computed result, due to neglect of electron correlation effects. Cluster calculations on $KNiF_3$ (Ref. 18), at the UHF and unrestricted second-order perturbation levels, show a correlation error of about -50% for the Hartree-Fock value of J, in broad agreement with our results.

Structure at variable pressure

The crystal structure of FeF_2 at room and high pressure was simulated by the calculation of the total energy at different unit-cell volumes, $E(V)$, for the ferromagnetic configuration with $P4_2/mnm$ space group. This choice was determined by the high computational cost of the antiferromagnetic state, and is justified by the ΔE(AF-FM) value being very small over the whole V range explored (e.g., it amounts to -2.2×10^{-4} hartree, for a -4% volume contraction with respect to the experimental value). Two structural degrees of freedom have to be taken into account: the c/a ratio of unit-cell edges, and the x (F) fractional coordinate, remembering that fluorine occupies the four positions $(\pm x,\pm x,0)$ and $(\frac{1}{2}\pm x,\frac{1}{2}\pm x,\frac{1}{2})$ in the unit cell. A full relaxation of c/a and x_F was performed for $\Delta V/V=-4$, 0, +4, +8%, deriving by polynomial least-squares approximations the $c/a(V)$ and $x_F(V)$ dependencies from the least-energy structure configurations. This allowed us to extrapolate the relaxation effect also to the -8% and $+12\%$ $\Delta V/V$ values. The $E(V)$ numerical curve obtained was interpolated by the Murnaghan equation of state,[19] deriving the $p(V)$ curve and transforming the volume dependence of lattice constants and fluorine coordinate into a pressure dependence. The whole procedure is described in detail elsewhere.[20] In Table II, the parameters of the Murnaghan formula (V_0, E_0, K_0, K_0') are reported, together with the

TABLE II. Theoretical (least-energy) and experimental equilibrium values of unit-cell edges (Å) and volume (Å^3), atomic fractional coordinates, selected interatomic distances (Å) and angles (°), elastic bulk modulus (GPa) and its pressure derivative, and total energy (hartree) for FeF_2. Percentage errors are indicated in parentheses.

	Theor.	Expt.
a_0	4.814 (+2.4%)	4.700[a]
c_0	3.339 (+0.9%)	3.310[a]
c_0/a_0	0.694 (−1.4%)	0.704
V_0	77.37 (+5.8%)	73.12
x(F)	0.3014	0.3013[a]
Fe-F	2.052 (+2.4%)	2.003×2
	2.148 (+1.5%)	2.117×4
Fe1-F-Fe1	102.0	102.8
Fe1-F-Fe2	129.0	128.6×2
K_0	106 (+6%)	100[b]
K_0'	3.7 (−20%)	4.65[b]
E_0	−1461.5087	

[a]Reference 15.
[b]Reference 12.

corresponding equilibrium (zero pressure) values of the structural variables at the athermal limit. Experimental results coming from room-temperature X-ray-diffraction[15] and static compression[12] experiments are given, too; extrapolation to $T=0$ K was not possible, because of lack of data at variable temperature. The theoretical unit-cell edges are slightly overestimated, as usual for Hartree-Fock results on crystals containing heavy atoms.[8] The Jahn-Teller distortion of the FeF_6 octahedron is well reproduced, with two short and four longer Fe-F distances.

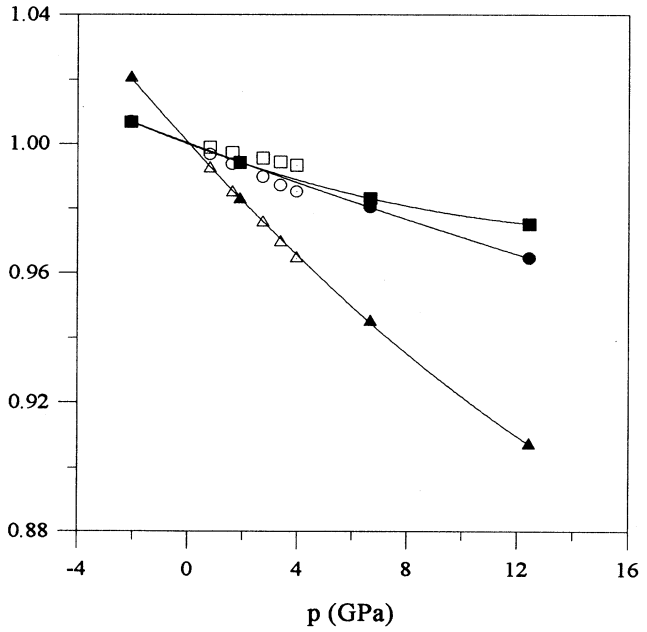

FIG. 1. Unit-cell constants of FeF_2, divided by their equilibrium values, plotted versus pressure. Circles, squares, and triangles indicate the a/a_0, c/c_0, and V/V_0 ratios, respectively. Closed and open symbols refer to calculated and experimental (Ref. 12) results, respectively.

The computed unit-cell edges and volume, divided by their equilibrium values, are plotted against pressure in Fig. 1. Some experimental points[12] are shown, too, for $p<4.5$ GPa. Indeed, above that pressure, iron fluoride appears to transform into a distorted fluorite-type structure;[12] thus, the simulation of the rutile structure in those conditions actually gives metastability curves, which could be useful to study the thermodynamics of the rutile/distorted fluorite transition. In the range where experimental data are available, the agreement with theoretical results appears to be excellent for the volume, while the compressibilities of c and a are slightly overestimated and underestimated, respectively. The observed increase of c/a with pressure is reproduced correctly; this shows that the structure is more easily compressed normally than parallel to the c axis, which corresponds to the direction of stronger linking of FeF_6 coordination octahedra. On the other hand, the longer Fe-F bond distance shows a larger compressibility (−3.4 TPa^{-1}) than the shorter one (−2.6 TPa^{-1}); these computed values compare well with the experimental ones (−3.2 and −2.3 TPa^{-1}, respectively).

ELECTRONIC PROPERTIES

Density of states and electron population

The electronic properties of antiferromagnetic FeF_2 can be discussed on the basis of the density of electron states (DOS) shown in Fig. 2 and of Mulliken population results for $\alpha+\beta$ and $\alpha-\beta$ electrons (Table III). The narrow peak at −30 eV in the DOS is due to 2s(F) atomic-like states; the valence band, ranging for 10 eV below the Fermi energy, shows a wide, complex shape of superposed p(F) and d^{α}(Fe1) [or d^{β}(Fe2)] states, and a spiky peak just below E_F due to d^{β}_{xy}(Fe1)- [or d^{α}_{xy}(Fe2)] electrons. In the conduction band, p(F) and d^{β}_{xz}(Fe1)+d^{β}_{yz}(Fe1) states overlap. A detailed representation of the valence bands is given in Fig. 3, where the wave-vector dependence of the one-electron energy eigenvalues is plotted along the [001] and [100] directions in reciprocal space. The very flat d^{β}_{xy}(Fe1) level appears clearly, close to the Fermi energy and well separated from the other eigenvalues at lower energies by a significant gap.

Thus, the main feature observed is the Jahn-Teller splitting of triply degenerate t^{β}_{2g}(Fe1) levels into a lower b^{β}_{2g} (d^{β}_{xy}) state, occupied by one electron per atom, and a higher pair of doubly degenerate e^{β}_{g} ($d^{\beta}_{xz}+d^{\beta}_{yz}$) empty states. This type of splitting is made possible by the tetragonal compressive deformation of the FeF_6 octahedron (two shorter and four longer Fe-F distances).[10] A stretched octahedron would have led to an energy inversion of $d^{\beta}_{xz}+d^{\beta}_{yz}$ with respect to d^{β}_{xy} states, so as to bring about a metallic rather than insulating electron configuration (unless the $d^{\beta}_{xz}+d^{\beta}_{yz}$ degeneracy would be lifted by the spin-orbit interaction). This analysis is

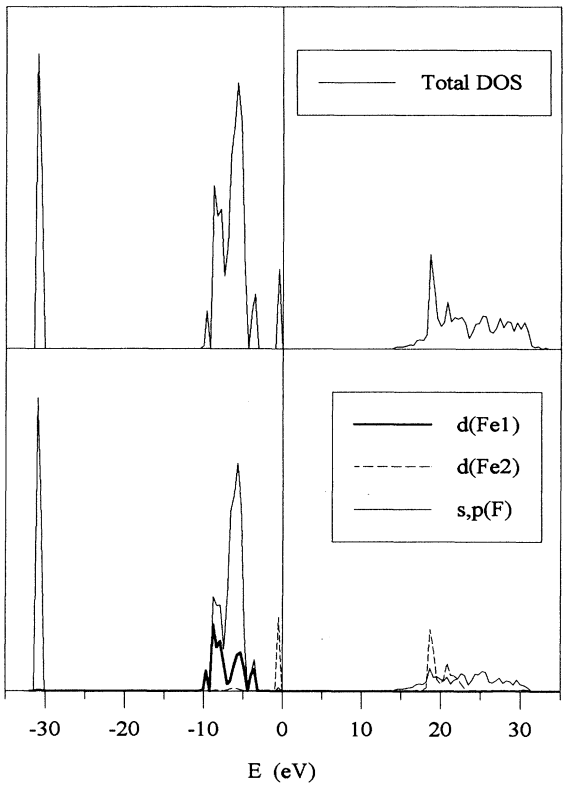

FIG. 2. DOS (density of electron states) of antiferromagnetic FeF_2 relative to spin-up electrons (above), with projections onto atomic-orbital contributions (below). The spin-down diagram would exchange the d(Fe1) and d(Fe2) projections, leaving the rest unvaried.

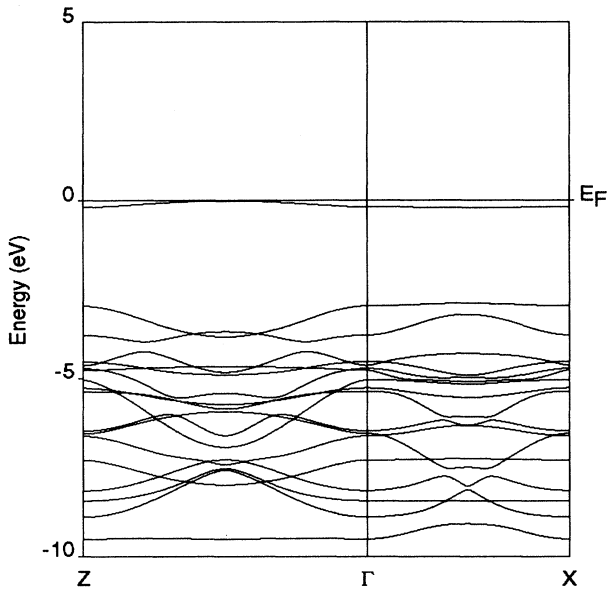

FIG. 3. Valence bands of antiferromagnetic FeF_2 projected along the [001] and [100] directions in reciprocal space.

confirmed by Mulliken population data, which show that 0.97 and 0.02 β electrons populate the d_{xy} and the $d_{xz}+d_{yz}$ orbitals of Fe1, respectively. As the valence-conduction band gap separates d(Fe) states, FeF_2 is a classic Mott-Hubbard insulator, unlike Fe_2O_3 which turns out to be a charge-transfer insulator.[8]

It should be remarked that in the LSDA calculation[4] no Jahn-Teller gap was opened inside the t_{2g}^{β} band, so that a metallic state appeared. It was necessary to introduce the GGA correction, accounting partially for the nonlocal nature of the spin-density functional, in order to reproduce the correct insulating behavior of FeF_2. This feature is simulated properly by our UHF calculation, though the entity of the gap is of course overestimated, as usual for band gaps in the Hartree-Fock approximation. The most evident difference between the GGA density of states[5] and the present one is that, in the former case, the p(F) band lies at lower energy than the d(Fe) one, with a gap in between. An intermediate situation is shown by the experimental x-ray photoelectron spectrum of FeF_2 (Ref. 21), where a wide band extends from the Fermi energy down to -12 eV, with two maxima at -5 and -8 eV ascribed to d(Fe) and p(F) states, respectively.

TABLE III. Mulliken population data ($|e|$) of electron charge distribution in atomic orbital shells ($\alpha+\beta$) and net atomic spins ($\alpha-\beta$) for Fe and F in antiferromagnetic FeF_2.

	Fe		F
	$\alpha+\beta$	$\alpha-\beta$	$\alpha+\beta$
Total sp	18.036	0.006	9.900
d_{z^2}	1.092	0.940	
$d_{x^2-y^2}$	1.045	0.978	
d_{xy}	1.966	0.030	
d_{xz}	1.011	0.990	
d_{yz}	1.011	0.990	
Total d	6.125	3.928	0.019
Grand total	24.161	3.934	9.019
Net charge	+1.839		−0.919

A further question concerns the possible Fe-F covalent bonding from interaction of d(Fe) and p(F) orbitals. The Fe-F Mulliken overlap population is hardly significant (0.003 $|e|$), so as to suggest a mainly ionic bonding. This is confirmed by the net charges on Fe and F (Table III), which are comparable to those of Mg (1.803 $|e|$) and F (-0.901 $|e|$) in MgF_2.[11] On the other hand, the small charge transfer of 0.16 $|e|$ from F^- to Fe^{2+} goes mostly (0.13 $|e|$) into the d (e_g) orbitals of Fe in the form of minority-spin electrons. A similar effect was also observed for Fe_2O_3.[8] Indeed, an appreciable negative Fe1-F bond population is observed for the spin density α-β (-0.021 $|e|$). This means that in the Fe1-F bonding region repulsion from α electrons (-0.009 $|e|$), but attraction from β ones ($+0.012$ $|e|$) arise, consistently with the β charge transfer referred to above; the opposite (β repulsion and α attraction) occurs in the Fe2-F case, confirming the Fe1-Fe2 superexchange interaction. The overall spin density of 3.93 $|e|$ on iron (Table III) shows a

reasonable consistency with the experimental magnetic moment of $3.75\mu_B$ (Ref. 14), which is similar to what was obtained in other cases.[7,8]

The present results can also be compared to those of a DV-$X\alpha$ calculation on the $[FeF_6]^{4-}$ cluster neutralized by a point-charge distribution.[22] A formalism at the molecular unrestricted HF level was used in that case, obtaining a slightly more covalent electron distribution than in our periodic case: z_{Fe} was 1.63 $|e|$, with the back-transferred 0.37 $|e|$ contributed as 0.13 and 0.24 $|e|$ into the 4s and d levels, respectively. Also for α-Fe_2O_3 (Ref. 8), a comparison with cluster-type calculations had given similar results, so that molecular approximations seem to overestimate covalency of bonding in crystalline systems.

Charge and spin densities

The overall features of chemical bonding and electronic structure of FeF_2 discussed above are confirmed by examining the charge- and spin-density maps. The planes $(1\bar{1}0)$ and (110) of the primitive tetragonal cell are considered. Deformation maps (crystal minus superposition of isolated ions) of the total $\alpha+\beta$ charge density are shown in Fig. 4, emphasizing the d-orbital Cartesian axes referred to the central Fe atom. The two maps are related by a shift of half the diagonal. The d_{xy}^2 configuration of Fe^{2+} in FeF_2 appears very clearly as β charge concentration along the lobes of the d_{xy} orbital and depletion from the d_{z^2} and $d_{x^2-y^2}$ lobes, with respect to the isolated ion, where the β electron is spherically distributed over all d orbitals. This deformation density of d_{xy} type is confirmed by maps on other planes, which are not reported here. Further, the charge around fluorine ions is distributed according to a sp^2-type triangular hybridization, consistently with the accepted view of chemical bonding in rutile-type structures.[23] Previous experimental x-ray-diffraction results[15] gave a deformation map resembling Fig. 4(a), but least-squares and multipole refinements were not able to discriminate between preferential occupation of d_{xy} or $d_{x^2-y^2}$ orbitals.

Maps of spin density for the antiferromagnetic structure appear in Fig. 5, and for the ferromagnetic case on the $(1\bar{1}0)$ plane only in Fig. 6. On iron, the spin density accumulates in directions different from those of the d_{xy} lobes, because the α and β components cancel just in the d_{xy} orbital. On fluorine, we observe a significant buildup of spin density in the FM case (Fig. 6), corresponding to 0.033 $|e|$ of the α-β Mulliken population. This effect is related to the net transfer of β electrons from F^- to Fe^{2+} and to the Fe-F bonding region, as discussed in the previ-

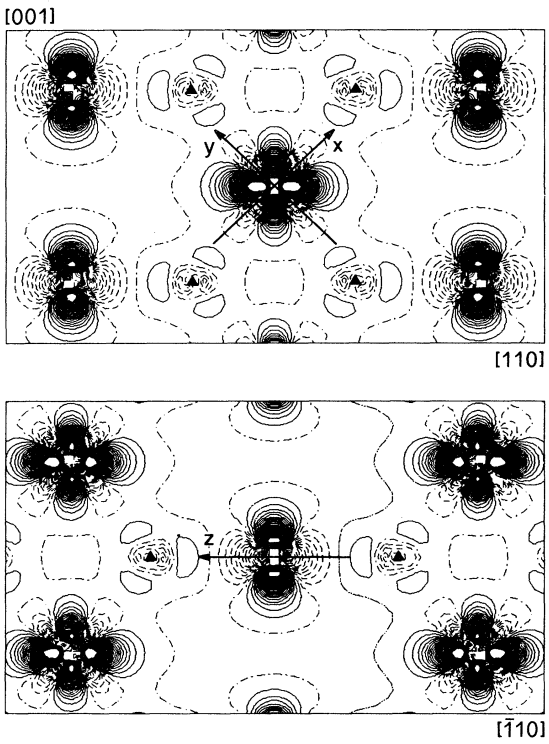

FIG. 4. Difference (crystal minus ionic superposition) charge-density maps on the $(1\bar{1}0)$ and (110) planes (above and below, respectively) for FeF_2. Triangles indicate the positions of F atoms. The reference axes for d orbitals on the Fe2 atom are shown. Isodensity curves are separated by 0.05 e Å^{-3}; continuous, dashed-dotted, and dashed lines indicate positive, zero, and negative values, respectively.

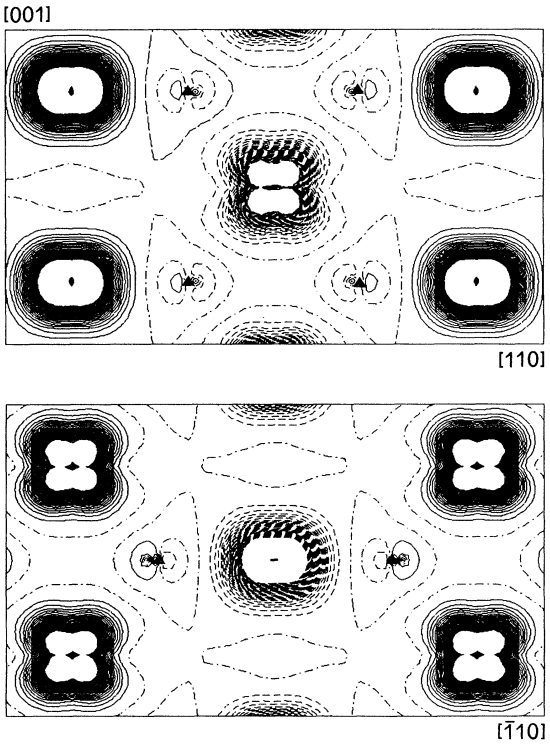

FIG. 5. Difference spin-density (spin-up minus spin-down) maps on the $(1\bar{1}0)$ and (110) planes (above and below, respectively) for antiferromagnetic FeF_2. Isodensity curves as in Fig. 4.

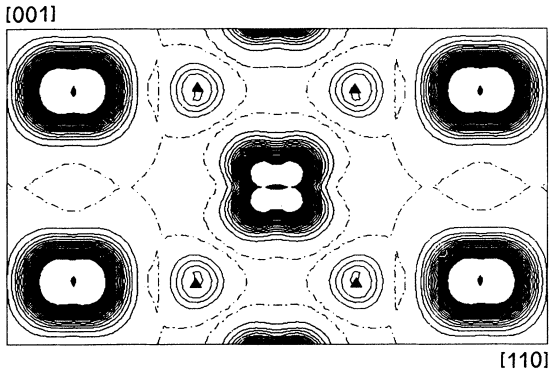

FIG. 6. Difference spin-density (spin-up minus spin-down) map on the $(1\bar{1}0)$ plane for ferromagnetic FeF_2. Isodensity curves as in Fig. 4.

ous section. In the AF case (Fig. 5), a smaller spin polarization on F^- occurs, too, but with opposite signs according to the majority spins of the neighboring iron ions. The β transfer from F to Fe1 leaves an excess of α electrons on F in the direction of Fe1, while the contrary occurs in the direction of Fe2. This is a pictorial evidence of the superexchange interaction between Fe1 and Fe2, via the diamagnetic ligand F.

CONCLUSIONS

The Jahn-Teller lifting of t_{2g} degeneracy for Fe^{2+} in tetragonal FeF_2 has been represented appropriately within the periodic unrestricted Hartree-Fock approximation. All other electronic properties are reproduced correctly, including the Mott-Hubbard insulator nature, at a level comparable to that attained by the DFT-LSDA-GGA scheme. We are thus confident that other, more complex types of degeneracy lifting in crystalline compounds of transition metals will be treated satisfactorily, too. Further, the method of calculation used seems to be particularly suitable to account for magnetic properties, as the antiferromagnetic character of FeF_2 could be simulated successfully despite the low Néel temperature. The results obtained for the equation of state and structural properties vs pressure throw light onto the crystal-chemical behavior of the rutile-type structure and can be possibly applied to the study of its phase transformations.

ACKNOWLEDGMENTS

The work was supported by the Human Capital and Mobility Programme of the European Union under Contract No. CHRX-CT93-0155, and by the Ministero Università e Ricerca Scientifica e Tecnologica, Roma.

[1]R. Dovesi, V. R. Saunders, and C. Roetti, *CRYSTAL92. User's Manual,* Gruppo di Chimica Teorica (Università di Torino, Torino, 1992).

[2]P. Blaha, K. Schwarz, and R. Augustyn, Computer Code WIEN93, Technical University of Vienna, 1993.

[3]E. Aprà, Ph.D. thesis, University of Torino, 1993. The UHF option will be included in a new release of the CRYSTAL code, CRYSTAL95, to be distributed at the end of 1995.

[4]P. Dufek, K. Schwarz, and P. Blaha, Phys. Rev. B **48**, 12 672 (1993).

[5]P. Dufek, P. Blaha, V. Sliwko, and K. Schwarz, Phys. Rev. B **49**, 10 170 (1994).

[6]M. D. Towler, N. L. Allan, N. M. Harrison, V. R. Saunders, W. C. Mackrodt, and E. Aprà, Phys. Rev. B **50**, 5041 (1994).

[7]W. C. Mackrodt, N. M. Harrison, V. R. Saunders, N. L. Allan, M. D. Towler, E. Aprà, and R. Dovesi, Philos. Mag. A **68**, 653 (1993).

[8]M. Catti, G. Valerio, and R. Dovesi, Phys. Rev. B **51**, 7441 (1995).

[9]J. M. Ricart, R. Dovesi, V. R. Saunders, and C. Roetti, Phys. Rev. B (to be published).

[10]K. I. Kugel' and D. I. Khomskii, Usp. Fiz. Nauk **136**, 621 (1982) [Sov. Phys. Usp. **25**, 231 (1982)].

[11]M. Catti, A. Pavese, R. Dovesi, C. Roetti, and M. Causà, Phys. Rev. B **44**, 3509 (1991).

[12]N. Nakagiri, M. H. Manghnani, Y. H. Kim, and L. C. Ming, *High-Pressure Research in Mineral Physics,* edited by M. H. Manghnani and Y. Syono (Terra Scientific Publishing Company, Tokyo, 1987), pp. 281–287.

[13]W. H. Hehre, L. Radom, P. R.Schleyer, and J. A. Pople, *Ab Initio Molecular Orbital Theory* (Wiley, New York, 1986).

[14]M. J. M. de Almeida and P. J. Brown, J. Phys. C **21**, 1111 (1988).

[15]M. J. M. de Almeida, M. M. R. Costa, and J. A. Paixão, Acta Crystallogr. Sect. B **45**, 549 (1989).

[16]P. W. Anderson, Solid State Phys. **14**, 99 (1963).

[17]L. J. de Jongh and R. Block, Physica **79B**, 568 (1975).

[18]J. A. Mejias and J. F. Sanz, J. Chem. Phys. **102**, 850 (1995).

[19]F. D. Murnaghan, Proc. Natl. Acad. Sci. USA **30**, 244 (1944).

[20]M. Catti, G. Valerio, R. Dovesi, and M. Causà, Phys. Rev. B **49**, 14 179 (1994).

[21]P. Kowalczyk, L. Ley, F. R. McFeely, and D. A. Shirley, Phys. Rev. B **15**, 4997 (1977).

[22]P. J. Brown, B. N. Figgis, and P. A. Reynolds, J. Phys. Condens. Matter **2**, 5297 (1990).

[23]P. I. Sorantin and K. Schwarz, Inorg. Chem. **31**, 567 (1992).